Synchronization of chaos in coupled systems

Meng Zhan,[1] Gang Hu,[2,1] and Junzhong Yang[3]
[1]*Department of Physics, Beijing Normal University, Beijing 100875, China*
[2]*China Center for Advanced Science and Technology (CCAST) (World Laboratory), P.O. Box 8730, Beijing 100080, China*
[3]*The James Franck Institute, the University of Chicago, 5640 South Ellis Avenue, Chicago, Illinois 60637*
(Received 28 January 2000; revised manuscript received 10 April 2000)

The stability of synchronous chaos of coupled oscillators with diffusive and gradient couplings is investigated. The stability boundaries of all transverse modes can be simultaneously drawn by justifying the boundary of a single mode, according to a scaling relation. Therefore, the distribution of stable and unstable regions can be explicitly shown in control parameter space. Bifurcations through different unstable modes, leading to different spatial orders, are analyzed.

PACS number(s): 05.45.−a

Recently, chaos synchronization has become a topic of great interest, due to its theoretical significance and practical applications [1–15]. There have been some theories dealing with the stability of synchronous chaotic states in coupled systems, like methods of master stability functions [11] and eigenvalue analysis [12,13]. However, they are all represented in the space of $\mathrm{Re}(\lambda)$ and $\mathrm{Im}(\lambda)$, with λ being the eigenvalues of coupling matrix, and not explicitly shown in a control parameter space. In this paper, we extend the scaling relation of Ref. [6], and investigate chaos synchronization of coupled systems directly in diffusive and gradient coupling parameter space, which is physically meaningful, and then the conditions and classifications for various types of bifurcations can be identified for well defined physical situations.

We consider N identical coupled nonlinear oscillators with nearest couplings and periodic boundary conditions,

$$\dot{u(j)} = f(u(j)) + (e+r)\Gamma(u(j+1)-u(j)) + (e-r) \times \Gamma(u(j-1)-u(j)), \qquad j = 1,2,\ldots,N, \tag{1}$$

where $u(j) \in R^n$, the function f is nonlinear and capable of exhibiting chaotic solutions, e and r are scalar diffusive and gradient coupling parameters, respectively, and Γ is a $n \times n$ constant matrix linking coupled variables. Such equations could represent a discrete reaction-diffusion equation with n species.

We are interested in bifurcations from synchronous chaotic states; these states reside on a synchronization manifold defined by $M = \{u(1) = u(2) = \ldots = u(N) = s(t)\}$, where the chaotic solution $s(t)$ satisfies the single oscillator equation $\dot{s(t)} = f(s)$. Stability of the synchronous state can be determined by linearizing Eq. (1) about $s(t)$. From the spatial Fourier transformation we can get the equation of spatial Fourier modes [6,13]

$$\dot{\eta_k} = (Df(s) + [\mathrm{Re}(\lambda) + i\,\mathrm{Im}(\lambda)]\Gamma)\,\eta_k, \tag{2a}$$

$$\mathrm{Re}(\lambda) = -4e\sin^2(\pi k/N),\ \mathrm{Im}(\lambda) = -2r\sin(2\pi k/N), \qquad k = 0,1,\ldots,N-1, \tag{2b}$$

where $Df(s)$ is the Jacobian of f on $s(t)$. Therefore the $k=0$ mode governs motion on the synchronized manifold and $k = 1,\ldots,N-1$ modes determine the stability of the synchronous state. If all these $N-1$ transverse modes are stable (i.e., corresponding to negative Lyapunov exponents), we can find the stable synchronous state, and we cannot do so, otherwise. Therefore, the stable synchronous chaotic region should be found in the overlap set of the stable regions of all these transverse modes.

In Ref. [13] some of the authors of the present paper analyzed the stable and unstable regions in the $\mathrm{Re}(\lambda)$–$\mathrm{Im}(\lambda)$ space, from which the bifurcation boundary in physically meaningful control parameter space (such as in $e-r$ space) is not clear, because with this method separate comparisons between all the eigenvalues of the coupling matrix with the distribution of the stability region is needed for determining the stability. In order to conveniently indicate the stability condition in $e-r$ space, let us study the structure of Eqs. (2). We define the largest transverse Lyapunov exponent (TLE) for the kth mode of N-particle system in Eqs. (2) as λ_N^k, which determines the stability boundary of this mode by $\lambda_N^k = 0$. The structure of Eq. (2b) gives a function relation between the TLE's for different mode number k and different system size N. In particular, for a given coupling matrix Γ, the TLE's of all modes can be obtained from the TLE as a single mode. Let us consider a mode of $k=1$ mode for $N=4$, where we have

$$\mathrm{Re}(\lambda) = -2e,\ \mathrm{Im}(\lambda) = -2r. \tag{3}$$

In this case, we can modify Eq. (2a) to

$$\dot{\eta_1} = (Df(s) - (2e+2r)\Gamma)\,\eta_1 \quad (N=4). \tag{4}$$

Then the stability analysis for this mode is directly shown in the physical parameter $e-r$ space. The main point of this paper is we can numerically compute Eq. (4) for determining the stability region of mode $k=1$ (also $k=N-1$) for $N=4$, then the stability boundaries for all other modes $k \neq 0$ can be drawn accordingly by applying the identities

$$\lambda_N^k(e,r)=\lambda_4^1(2e\sin^2(\pi k/N),r\sin(2\pi k/N)). \quad (5)$$

This implies a simple scaling transformation of the stability region of λ_4^1 in both e and r axes, which is a direct extension of Eq. (4) in Ref. [6].

Numerical computation can be conducted as follows: First, from Eq. (4) we can get the critical curve identifying the stable region in the $e-r$ plane for the $k=1$ mode of the $N=4$ system, that is, the largest TLE of this mode crosses zero at the critical line, which can be done only numerically. Then we can obtain critical curves for all other modes and for arbitrary N by applying the scaling transformation, Eq. (5), for both abscissa and ordinate of the (e,r) space. For stabilizing the synchronous chaotic state, we should require all transverse modes $(k\neq 0)$ to be stable, therefore in the (e,r) space the region of stable synchronous chaos corresponds to the overlap set of the stable regions of all transverse modes.

To show the above analysis we take the coupled Lorenz oscillators as our example, where the extension to other general coupled systems is straightforward. The single Lorenz system reads

$$\dot{x}=\sigma(y-x),$$

$$\dot{y}=\rho x-y-xz, \quad (6)$$

$$\dot{z}=xy-\beta z,$$

where $\sigma=10$, $\beta=1.0$, and $\rho=28.0$, at these parameters the motion is chaotic. We use Eq. (6) as the local dynamics of the coupled system, Eq. (1), and consider different linking matrix Γ's.

In Figs. 1(a), 1(b), and 1(c) we show three kinds of critical curves of types I, II, and III for the $k=1$ mode of $N=4$ in the (e,r) space for the linking matrices

$$\Gamma=\begin{pmatrix}0&0&0\\1&0&0\\0&0&0\end{pmatrix}, \quad \begin{pmatrix}0&0&0\\0&1&0\\0&0&0\end{pmatrix},$$

and

$$\begin{pmatrix}0&1&0\\0&0&0\\0&0&0\end{pmatrix},$$

respectively. The critical lines are justified by numerically computing the linear equations (4) for zero largest Lyapunov exponent, and the words ''Unstable'' and ''Stable'' indicate unstable and stable regions of this mode, respectively.

In Figs. 2–4 we predict the stable regions for different k and N by applying the scaling relation of Eq. (5) and by considering the stable regions of Figs. 1(a)–1(c), respectively. The overlaps of all those stable regions are just the regions for the stable synchronous chaotic state, indicated by dotted regions.

From Figs. 2–4 the instability condition, bifurcation modes, and the different bifurcation features for the three kinds of instability distributions become apparent. First, we

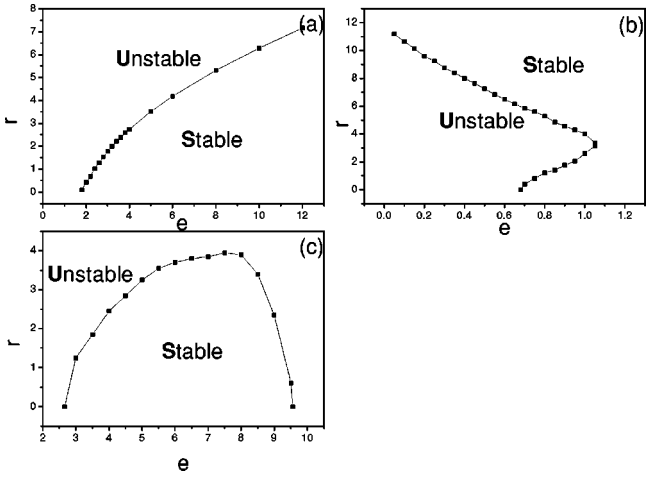

FIG. 1. (a), (b), (c). The three kinds of type I, II, and III critical curves of system, Eq. (1) with local dynamics, Eq. (5), for $N=4$ and $k=1$ mode, plotted in the (e,r) space. $\sigma=10$, $\beta=1.0$, $\rho=28.0$ (which will be used for all the following figures).

$$\text{(a)}\ \Gamma=\begin{pmatrix}0&0&0\\1&0&0\\0&0&0\end{pmatrix}; \quad \text{(b)}\ \Gamma=\begin{pmatrix}0&0&0\\0&1&0\\0&0&0\end{pmatrix},$$

and (c)

$$\Gamma=\begin{pmatrix}0&1&0\\0&0&0\\0&0&0\end{pmatrix}.$$

may ask can we stabilize the synchronous chaos for sufficiently large system $N\gg 1$ by varying the diffusive and gradient couplings e and r? The answer is: for type I distribution [Figs. 1(a) and 2], we can do so by increasing the diffusive coupling e, then the stable region always appears for small gradient coupling r; for type II distribution [Figs. 1(b) and 3], we can also do so by increasing e, while the stable regions appear for both small and large r (or for any r if e is larger than a certain value); however, for type III distribution [Figs. 1(c) and 4], there is a critical system size N_c, above which the synchronous chaos cannot be stabilized whatever e and r. For instance, in the case of Fig. 4, no stable synchronization can be found in any $e-r$ region for $N>5$, because the overlap set of the stable regions of transverse modes is empty.

Second, for type I distribution the stable synchronous chaos can be destabilized only by long wave mode $(k=1)$ for any N (Fig. 2); while for both types II and III distributions the homogeneous state can be desynchronized by both long wave $(k=1)$ and short wave $[k=N/2$ if N is even number, or $k=(N-1)/2$ if N is odd one] instabilities (Figs. 3 and 4).

The most significant point is that Figs. 2 –4 predict not only the bifurcation parameters, but also the spatiotemporal features of the motion after the instability of the synchronous chaos. In Ref. [13], Hu, Yang, and Liu found a Hopf bifurcation from chaos for the type I distribution, i.e., an oscillation with typical frequency can be associated with the desyn-

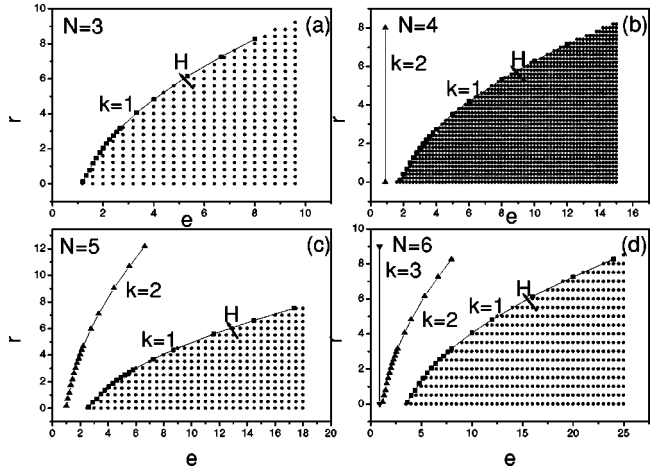

FIG. 2.

$$\Gamma=\begin{pmatrix}0&0&0\\1&0&0\\0&0&0\end{pmatrix}.$$

The stable regions for different system size and different transverse modes. The overlap of stable regions of all transverse modes is the region of stable synchronous state, denoted by dotted regions. By crossing the instability boundary through arrow H, we can observe Hopf bifurcation from synchronous chaos.

chronization element after the instability of the synchronous chaos. In Figs. 2 and 3 we find this kind of bifurcation exists rather generally (see the arrows indicated by H), where two modes (k and $N-k$ for $k\neq N/2$) turn to be unstable simultaneously. In Ref. [6], Heagy, Pecora, and Carroll revealed a kind of short wave bifurcation, which can be easily found in Figs. 3 and 4 (see the arrows indicated by S).

In this paper, we focus on short wave bifurcation. In Figs.

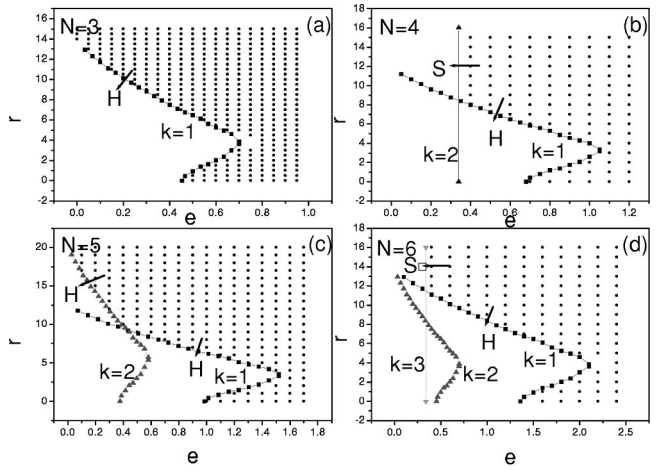

FIG. 3. The same as Fig. 2 with Γ replaced by

$$\Gamma=\begin{pmatrix}0&0&0\\0&1&0\\0&0&0\end{pmatrix}.$$

By crossing the instability boundary through arrows H and S we can observe Hopf bifurcation and short wave bifurcation from synchronous chaos, respectively.

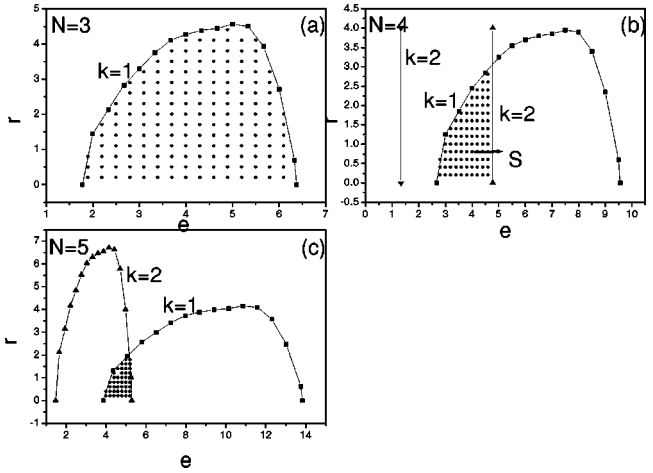

FIG. 4. The same as Fig. 2 with Γ replaced by

$$\Gamma=\begin{pmatrix}0&1&0\\0&0&0\\0&0&0\end{pmatrix}.$$

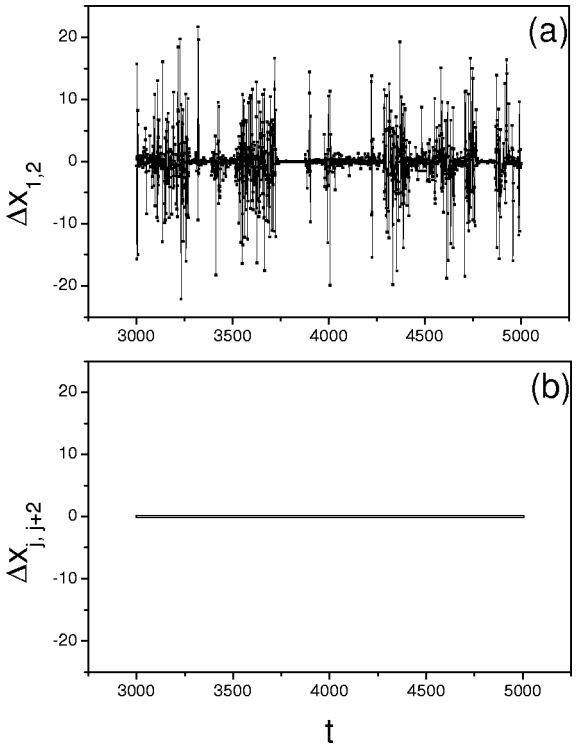

FIG. 5. The spatial order after short wave bifurcation.

$$\Gamma=\begin{pmatrix}0&0&0\\0&1&0\\0&0&0\end{pmatrix},$$

$e=0.3$, $r=14.0$ [see the square open point in Fig. 3(d)]. The system state has the following characteristic: $x_1(t)=x_3(t)=x_5(t)=a(t)$, $x_2(t)=x_4(t)=x_6(t)=b(t)$. Thus we have $ababab$ spatial order: (a) $\Delta X_{1,2}$ vs t; (b) $\Delta X_{j,j+2}(j=1,2,3,4)$ vs t.

3 and 4, when we cross the instability boundaries by following the arrows S, a single mode $k=N/2$ can become unstable, indicating short wave instability. In Ref. [6] Heagy, Pecora, and Carroll addressed this type of instability and found periodic oscillations with smallest spatial scale after short wave bifurcation. In our cases, we find chaotic motion with smallest spatial scale, i.e., short wave bifurcation between two different chaotic states. This phenomenon is regarded as new and significant. Now let us consider the state variation along the arrow S in Fig. 3(d). In the dotted region, synchronous chaos is stable. After crossing the instability boundary through arrow S we examine the system state at $e=0.3$, $r=14.0$ (indicated by a square). We find an interesting state: all oscillators perform chaotic motions, and the six oscillators form two groups: $x_1(t)=x_3(t)=x_5(t)$ (state a) and $x_2(t)=x_4(t)=x_6(t)$ (state b), the motion shows on–off intermittency between these two groups a and b. In Fig. 5(a) we plot $\Delta X_{1,2}$ vs t, and observe typical on–off intermittency; in Fig. 5(b) we present $\Delta X_{j,j+2}(j=1,2,3,4)$ vs t, which is identically equal to zero, indicating synchronization. Therefore, as the synchronous chaos is desynchronized with unstable mode $k=N/2$, we find the partially synchronized chaotic state in the form of $ababab$. This smallest spatial scale reasonably corresponds to the short wave instability ($ababab$ structure indicates three spatial periods, indicating $k=3$ for $N=6$).

In summary, we have investigated the chaos synchronization problem of coupled chaotic oscillators with both diffusive and gradient couplings. By applying the scaling relation, Eq. (5), we are able to draw instability boundaries for all transverse modes from that of a single mode. Thus the distribution of stable and unstable regions of the synchronous chaos can be explicitly shown in the physically meaningful control parameter space. From this distribution the instabilities for different modes can be predicted, and the spatial orders after different mode bifurcations, in particular, Hopf bifurcation and short wave bifurcation from synchronous chaos, can be classified.

This research was supported by the National Natural Science Foundation of China, the Nonlinear Science Project of China, and the Foundation of Doctoral Training of Educational Bureau of China.

[1] L.M. Pecora and T.L. Carroll, Phys. Rev. Lett. **64**, 821 (1990).
[2] J.F. Heagy, T.L. Carroll, and L.M. Pecora, Phys. Rev. Lett. **73**, 3528 (1994).
[3] Y.-C. Lai, C. Grebogi, J.A. Yorke, and S.C. Venkataramani, Phys. Rev. Lett. **77**, 55 (1996).
[4] S.C. Venkataramani, B.R. Hunt, and E. Ott, Phys. Rev. E **54**, 1346 (1996).
[5] J.F. Heagy, T.L. Carroll, and L.M. Pecora, Phys. Rev. E **50**, 1874 (1994).
[6] J.F. Heagy, L.M. Pecora, and T.L. Carroll, Phys. Rev. Lett. **74**, 4185 (1995).
[7] L.M. Pecora, Phys. Rev. E **58**, 347 (1998).
[8] M.A. Zaks, E.-H. Park, M.G. Rosenblum, and J. Kurths, Phys. Rev. Lett. **82**, 4228 (1999).
[9] M.A. Matias and J. Guemez, Phys. Rev. Lett. **81**, 4124 (1998).
[10] G. Hu, J.Z. Yang, W.Q. Ma, and J.H. Xiao, Phys. Rev. Lett. **81**, 5314 (1998).
[11] L.M. Pecora and T.L. Carroll, Phys. Rev. Lett. **80**, 2109 (1998).
[12] J.Z. Yang, G. Hu, and J.H. Xiao, Phys. Rev. Lett. **80**, 496 (1998).
[13] G. Hu, J.Z. Yang, and W.J. Liu, Phys. Rev. E **58**, 4440 (1998).
[14] G. Hu, F.G. Xie, Z.L. Qu, and P.L. Shi, Commun. Theor. Phys. **31**, 99 (1999).
[15] P.L. Shi, G. Hu, and L.M. Xu, Acta Phys. Sin. **49**, 1,24 (2000).